



CHALMERS
UNIVERSITY OF TECHNOLOGY

A simple way of improving graphite nanoplatelets (GNP) for their incorporation into a polymer matrix

Downloaded from: <https://research.chalmers.se>, 2025-06-02 10:31 UTC

Citation for the original published paper (version of record):

Persson, H., Yao, Y., Klement, U. et al (2012). A simple way of improving graphite nanoplatelets (GNP) for their incorporation into a polymer matrix. *Express Polymer Letters*, 6(2): 142-147. <http://dx.doi.org/10.3144/expresspolymlett.2012.15>

N.B. When citing this work, cite the original published paper.

A simple way of improving graphite nanoplatelets (GNP) for their incorporation into a polymer matrix

H. Persson*, Y. Yao, U. Klement, R. W. Rychwalski

Chalmers University of Technology, Department of Materials and Manufacturing Technology, Göteborg, Sweden

Received 30 May 2011; accepted in revised form 13 September 2011

Abstract. A simple method of solvent exfoliation/refining of direct-graphite nanoplatelets for their better incorporation into a polymer matrix is presented. We demonstrate the method for polystyrene. The method relies on sonication in N-methyl-2-pyrrolidone solvent, with surfactant assistance. A small amount of polystyrene is added to the solvent in order to increase the viscosity, this enhancing the exfoliation process and resulting in formation of a polymeric layer on graphene for its better incorporation in the polymer matrix. Polystyrene-coated thin graphene stacks form a stable dispersion, while thicker graphite nanoplatelets settle out. Thus bulk separation of thin and thick graphene stacks takes place.

The polystyrene-coated thin graphene stacks are studied using Transmission Electron Microscopy in two ways: (i) we calculate the number of graphene layers forming thin graphene stacks, and (ii) we employ Selected Area Diffraction to confirm our image analysis results by checking the intensity ratio (1100) and (2100) deflections in the diffraction patterns. Five layers is found to be the cut-off number, that is there are no stacks >5 layers, and 3 layer stacks are dominantly present. The average largest in-plane dimension is found to be approximately 2.5 μm (reduction by 50%).

Keywords: nanocomposites, solvent dispersion, graphene

1. Introduction

Graphene has triggered off further expectations in nanocarbon polymer composites, and enthusiasm in the research community. However, at present, only minute amounts of single monolayer graphene from ‘bottom-up’ production is available. For nanocomposites, massive amounts of graphene is needed. In our work we use direct-graphite nanoplatelets (GNP), now becoming increasingly available. Attractiveness of the material stems among others from the low cost of graphite, the precursor for GNP. Indeed, price of GNP is low compared to e.g., multi-wall carbon nanotubes (MWNT). It is well known that the quality of polymer nanocomposites hinges on the quality of the filler. In the case of graphene based filler, this first of all refers to well-defined and small thickness.

The need for well-defined exfoliated GNP has been emphasized in the literature, and efficient ways to address the problem have been presented. Green and Hersam [1, 2] used density gradient ultracentrifugation, and achieved separation in graphene stacks by the number of layers. Sun *et al.* [3] used density gradient ultracentrifugal rate separation, and achieved sorting by sheet size and surface chemistry. In above works, a density gradient is essential, although in report [3] results for a uniform medium column are also included. The authors prepared a separate external measuring uniform density column, and found that separation was achievable over a smaller size range. Methods to exfoliate powdered graphite have been developed by Coleman and collaborators, among others in [4, 5], and by Bourlinos *et al.* [6], as well as Blake *et al.* [7].

*Corresponding author, e-mail: henrik.persson@chalmers.se
© BME-PT

Simultaneously, research into various types of graphite nanoplatelets, such as graphene oxide (GO) [8, 9], chemically modified graphene [10], and thermally expanded graphite [11], as a precursor to graphene-based materials is carried out, and important results are published. The present state of knowledge of graphene-based materials/graphite nanoparticles, including preparation of polymer composites has been overviewed, *e.g.*, by Kim *et al.* [12], and Potts *et al.* [13].

In the present work, we proceed from the above experiences for graphite powder exfoliation, and adapt and modify them towards GNP exfoliation. We refine GNP material using solvent dispersion, where a small amount of polymer is added to the solvating medium. Direct-GNP microagglomerates are refined, nanoplatelets are exfoliated and polymer is deposited on graphene. The refined filler can easily be turned into a composite either by evaporating the solvent and using it as a masterbatch, or polymer could be added to the solution before solvent evaporation in order to tailor the filler content. To the best of our knowledge, there is no report on the use of polymer coated direct-graphite refining.

2. Experimental

2.1. Solvent dispersion

Our early unsuccessful trials included the use of toluene (after bath sonicating for 4 h, the entire mass of GNP material rapidly settled out). Then N-methyl-2-pyrrolidone (NMP) was used, and the following preparation was carried out.

GNP, xGnP from XG Sciences, USA, was mixed together with polyethylene glycol p-(1,1,3,3-tetramethylbutyl)-phenyl ether surfactant, Triton X-100 from Alfa Aesar, Germany, and NMP, in proportion 10:1:200 by weight (nanoplatelets:surfactant:solvent). The mixture was stirred for 15 minutes, and then sonicated in a cuvette in a bath for 2 hours (Branson 1510E-MTH, Branson Ultrasonic Corp., USA). The temperature in the bath did not exceed 55°C during the sonication.

We decided to increase the solvent viscosity by adding polystyrene (PS) (Polystyrol 143 E, BASF, Germany), which was first dissolved in NMP, in proportion 1:15 by weight. The PS-solution was then added to the GNP mixture, stirred for 30 minutes followed by additional sonication for 2 hours. The final concentration of GNP in the solution was

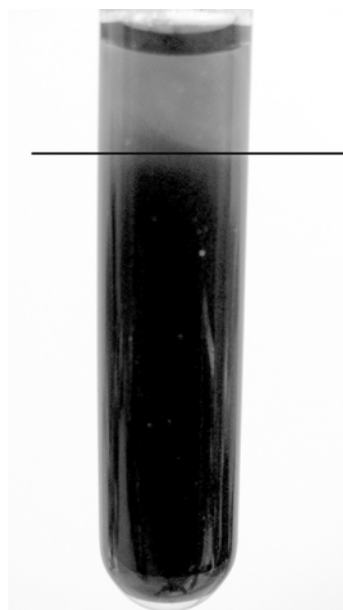


Figure 1. Stable dispersion of thin graphene stacks in NMP/PS (after sonication time of 4 h, and sedimentation time of 170 h)

5 wt% with respect to PS. Cavitations caused by sonication lead to initial intercalation and in turn facilitate solvent penetration into nanoplatelet. Increased solvent viscosity (by the presence of polymer) creates larger forces hindering reverse of intercalation. After 4 h of sonication, the dispersion in the cuvette appeared dark/black. After sedimentation time of close to 170 h, sediment settled out, and a dispersion appearing gray/tinted formed in the upper part of the cuvette (Figure 1), with a thin black layer floating on the surface. Using a microsyringe, a subset of the dispersion was carefully removed, avoiding the floating layer and the sediment.

2.2. Thermal gravimetric analysis

The subset was next analysed using Thermal Gravimetric Analysis (TGA) (TGA/DSC 1 Star system, Mettler Toldedo, Switzerland). The following program was used during the analysis, heating from 50–600°C at a rate of 20°C/min under nitrogen atmosphere, followed by a 40 min isothermal step at 600°C under air atmosphere, and then heating to 900°C at 20°C/min under air atmosphere. Star software v9.20 was used.

2.3. Transmission Electron Microscopy

The dispersion was further diluted 10 times in (NMP), and a small amount was deposited onto holey carbon grids (400 mesh), and then studied by

Transmission Electron Microscopy (TEM). Images and electron diffraction were taken with an electron transmission microscope (Zeiss EM912 Omega, Germany) equipped with an Ω energy filter and operated at 120 keV.

3. Results and discussion

3.1. TGA

In Figure 2, a representative measured TGA plot is shown. A pronounced weight loss starting at about 400°C originating from the degradation of the PS is clearly present. By applying oxygen containing atmosphere the remaining GNP was burnt off, and the GNP content was measured to be 0.13 wt% of that of the PS. This corresponds to a GNP concentration in the solution of 0.08 mg/ml, which is comparable to the results obtained by Khan *et al.* [4] at similar sonication time.

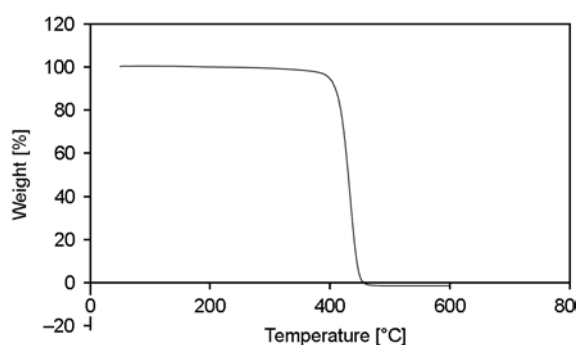


Figure 2. TGA plot of GNP/PS composite

3.2. TEM image analysis

Image analysis was carried out on 23 images. An example is shown in Figure 3.

As can be seen in Figure 3, distinguishable layers (shown with thin arrows) form a stack. Layers grayscale and boundary/edges made it possible to count the layers per stack, as proposed in [4]. Herein, PS molecules deposited on graphene facilitates image analysis, for example edges become more marked and contrasting. On the other hand, the deposited polymer disturbs imaging because of the extra background. Presence of polymer can be noticed on the holey carbon substrate; particularly the smallest hole is filled. Clearly, the layers do not overlap ideally, and the number of layers varies depending on location. In Figure 3, the maximum number of layers is 3. In Figure 4 (histogram), statistics summarizing the 23 images is given. We report

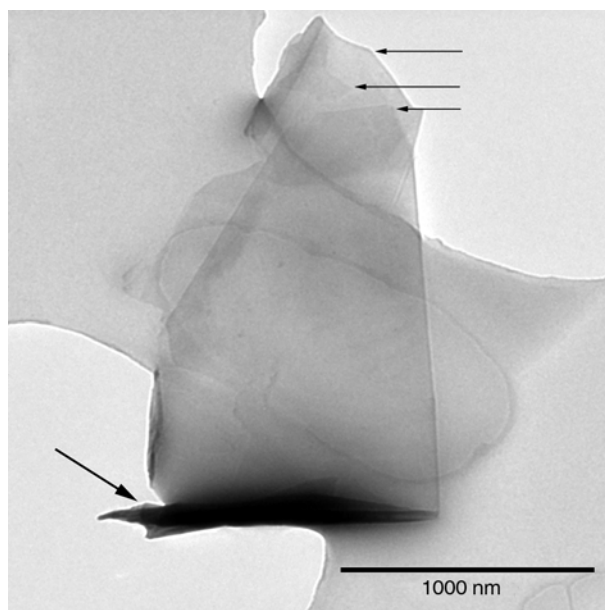


Figure 3. TEM image of a multilayer graphene stack. Thin arrows indicate the edges of the individual layers, and the bold arrow indicates a folded off-plane fragment of layer.

the maximum number of layers per stack. 5 layers is found to be the cut-off number. No stacks >5 layers were found, and 3 layer stacks are dominantly present. This is close to the statistics given in [4], using the edge-counting method proposed by the authors, for the case of exfoliating powdered graphite.

When computing the layers, occasionally, we needed to account for folded graphene. A folded off-plane fragment of layer is seen in Figure 3 (bold arrow). In such a case, two layers were counted. Also in Figure 3, a black grayscale domain can be seen. We believe this can be ascribed to carbon wrap containing polymer and surfactant molecules. In-plane dimensions of layers/stacks are reduced compared to that of pristine GNP, as specified by the supplier. The average largest in-plane dimension is found to

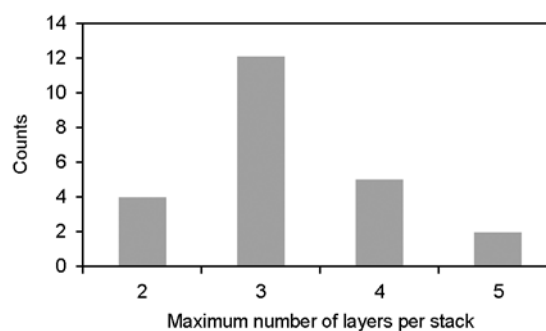


Figure 4. Histogram showing the maximum number of layers within a stack

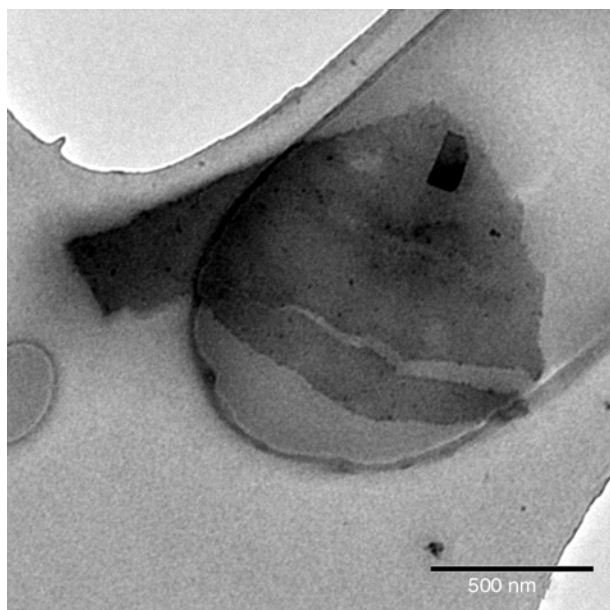


Figure 5. TEM image showing a layer containing a crack

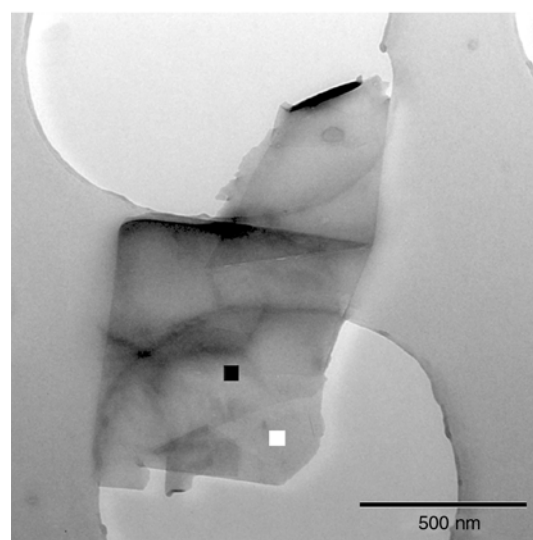
be approximately 2.5 μm . We ascribe this to the sonication process. A layer containing a crack, most likely developed during sonication, is seen in Figure 5. We note that on one occasion, one very large microagglomerate was observed.

3.3. Diffraction analysis

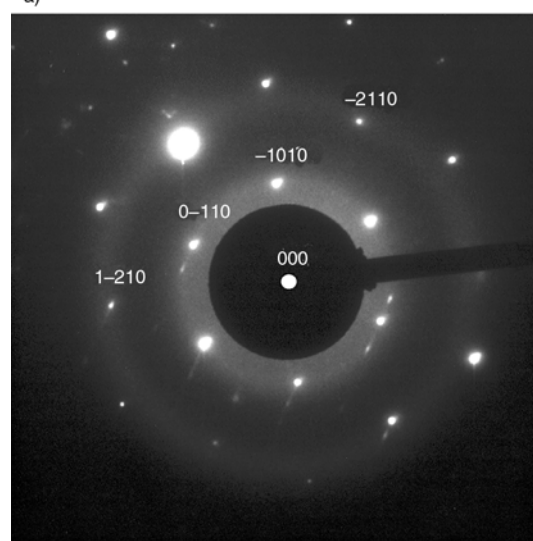
Electron diffraction was carried out as a complementary method, in addition to the image analysis described above. SAD and nano diffraction under Köhler illumination were performed using a small selected area aperture and condenser aperture with diameter of 5 μm .

The PS deposition requires caution when studying the graphene architecture; on the one hand the extra background, and on the other hand the additional irregular edges from PS presence, make subtle differences in identifying graphene edges. According to the numerical simulation with Fourier transformation of projected atomic potentials and scattering factors [14], the intensity ratio $I_{(1100)}/I_{(2100)}$ in the electron diffraction pattern of graphite/graphene with ABAB stacking can be used for distinguishing monolayer from multilayer graphene stacks, as follows.

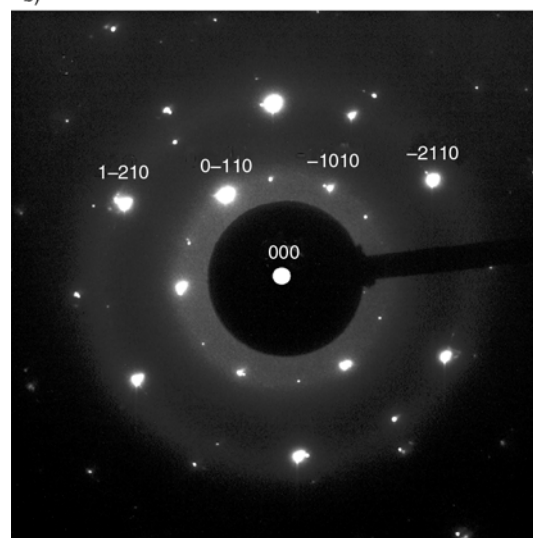
In Figure 6, TEM bright field image (a), and typical diffraction patterns taken from the monolayer region (b) (marked with a white dot), and multilayer region (c) (marked with a black dot) of a graphene stack, are shown. The image was sufficiently defocused in order to enhance the phase contrast of the



a)



b)



c)

Figure 6. a) TEM bright field image of graphene stack. b) SAD pattern taken from region marked in figure a) with the white dot (monolayer). c) SAD pattern taken from region marked in figure a) with the black dot (multilayer).

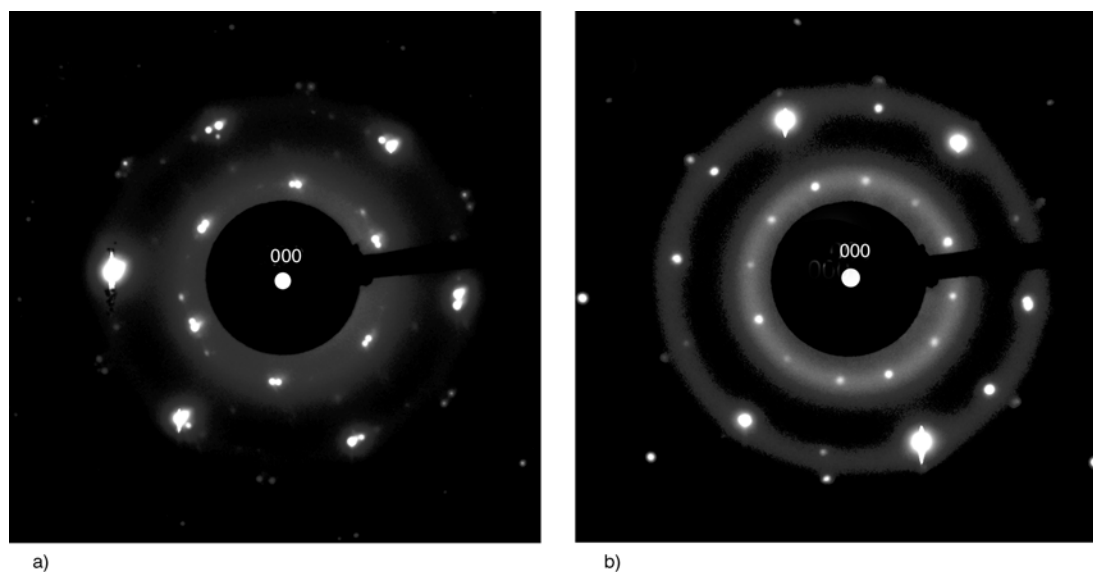


Figure 7. a) SAD pattern of two graphene sheets stacking with a rotation angle of 2.5° . b) SAD pattern of two multilayer graphene superimposed with a rotation angle of 30° .

image. The diffraction patterns exhibit the typical six-fold symmetry, which can be indexed as the [0001] zone pattern of graphite/graphene. As can be seen clearly, the spots intensity ratio $I_{(1100)}/I_{(2100)}$ is >1 in the monolayer pattern (Figure 6b), whereas $I_{(1100)}/I_{(2100)}$ is <1 in the multilayer pattern (Figure 6c). The observation is consistent with the result for pure graphene suspension [15]. The diffraction pattern in Figure 6c can be observed in nearly all the examined multilayer objects. Caution is needed when identifying a monolayer from TEM images. Some monolayer-looking objects may not be monolayer graphene, and have a diffraction pattern of multilayer. Thin graphite sheets or stacked graphene fragments may be mistaken for monolayer graphene particularly when covered with polymer molecules merging the individual edges into one single edge. The presence of monolayer regions and multilayer regions shown with SAD supports the statistical results in Figure 3, and thus we believe that the pristine GNPs have been successfully refined.

Another observation relates to the graphene stack schedule (or build-up), particularly random or non-random assembly. We find that they do not overlap or fold together randomly in the graphene/PS composite. Graphene sheets usually form stacks with either a very small rotation angle ($<5^\circ$) or close to 30° . Figure 7a presents a SAD pattern of graphene sheets stacking with a rotation angle of 2.5° . Figure 7b shows two sets of [0001] zone patterns super-

imposed of two multilayer graphene with a rotation angle of 30° . The latter rotation relationship can be often observed directly from folded edge of graphene sheets in images (Figure 6a and 6c). The stacking arrangements of the graphene sheets observed in this work are comparable to the zigzag and arm-chair chiralities in carbon nanotubes [16]. While the graphene stacks long range assembly is driven by the surface energy, we believe that when they meet, likely, the thin PS film remaining between the graphene sheets enables more mobility. As a result, the graphene sheets can rotate or orientate themselves towards favourable configurations, at lower energy states.

4. Conclusions

A simple method to exfoliate/refine direct-graphite nanoplatelets towards their better incorporation into a polymeric matrix is presented, and demonstrated for the case of polystyrene. By adding a small amount of polystyrene to N-methyl-2-pyrrolidone solvent containing surfactant, the solvent viscosity increased, and thus created larger forces during sonication and hindered the reverse of intercalation. The refined nanoplatelets were characterized by using Transmission Electron Microscopy based imaging and diffraction analysis. Using the edge-counting method, no platelets thicker than 5 layers, and dominantly 3-layer thick stacks were observed. The average layer's in-plane dimension was $2.5 \mu\text{m}$.

The presence of monolayer and multilayer regions, analysed with the selected area diffraction method supports the results.

Acknowledgements

Erik Nilsson at Swerea IVF is acknowledged for TGA measurements. The financial support from the Swedish Foundation for Strategic Research (SSF) is acknowledged.

References

- [1] Green A. A., Hersam M. C.: Solution phase production of graphene with controlled thickness via density differentiation. *Nano Letters*, **9**, 4031–4036 (2009). DOI: [10.1021/nl902200b](https://doi.org/10.1021/nl902200b)
- [2] Green A. A., Hersam M. C.: Emerging methods for producing monodisperse graphene dispersions. *Journal of Physical Chemistry Letters*, **1**, 544–549 (2010). DOI: [10.1021/jz900235f](https://doi.org/10.1021/jz900235f)
- [3] Sun X., Luo D., Liu J., Evans D. G.: Monodisperse chemically modified graphene obtained by density gradient ultracentrifugal rate separation. *ACS Nano*, **4**, 3381–3389 (2010). DOI: [10.1021/nn1000386](https://doi.org/10.1021/nn1000386)
- [4] Khan U., O'Neill A., Lotya M., De S., Coleman J. N.: High-concentration solvent exfoliation of graphene. *Small*, **6**, 864–871 (2010). DOI: [10.1002/smll.200902066](https://doi.org/10.1002/smll.200902066)
- [5] Hernandez Y., Nicolosi V., Lotya M., Blighe F. M., Sun Z., De S., McGovern I. T., Holland B., Byrne M., Gun'Ko Y. K., Boland J. J., Niraj P., Duesberg G., Krishnamurthy S., Goodhue R., Hutchison J., Scardaci V., Ferrari A. C., Coleman J. N.: High-yield production of graphene by liquid-phase exfoliation of graphite. *Nature Nanotechnology*, **3**, 563–568 (2008). DOI: [10.1038/nnano.2008.215](https://doi.org/10.1038/nnano.2008.215)
- [6] Bourlino A. B., Georgakilas V., Zboril R., Steriotis T. A., Stubos A. K.: Liquid-phase exfoliation of graphite towards solubilized graphenes. *Small*, **5**, 1841–1845 (2009). DOI: [10.1002/smll.200900242](https://doi.org/10.1002/smll.200900242)
- [7] Blake P., Brimicombe P. D., Nair R. R., Booth T. J., Jiang D., Schedin F., Ponomarenko L. A., Morozov S. V., Gleeson H. F., Hill E. W., Geim A. K., Novoselov K. S.: Graphene-based liquid crystal device. *Nano Letters*, **8**, 1704–1708 (2008). DOI: [10.1021/nl080649j](https://doi.org/10.1021/nl080649j)
- [8] Lee S. H., Dreyer D. R., An J., Velamakanni A., Piner R. D., Park S., Zhu Y., Kim S. O., Bielawski C. W., Ruoff R. S.: Polymer brushes via controlled, surface-initiated atom transfer radical polymerization (ATRP) from graphene oxide. *Macromolecular Rapid Communications*, **31**, 281–288 (2010). DOI: [10.1002/marc.200900641](https://doi.org/10.1002/marc.200900641)
- [9] Dreyer D. R., Park S., Bielawski C. W., Ruoff R. S.: The chemistry of graphene oxide. *Chemical Society Reviews*, **39**, 228–240 (2010). DOI: [10.1039/B917103G](https://doi.org/10.1039/B917103G)
- [10] Stankovich S., Dikin D. A., Dommett G. H. B., Kohlhaas K. M., Zimney E. J., Stach E. A., Piner R. D., Nguyen S. T., Ruoff R. S.: Graphene-based composite materials. *Nature*, **442**, 282–286 (2006). DOI: [10.1038/nature04969](https://doi.org/10.1038/nature04969)
- [11] Ansari S., Giannelis E. P.: Functionalized graphene sheet–Poly(vinylidene fluoride) conductive nanocomposites. *Journal of Polymer Science Part B: Polymer Physics*, **47**, 888–897 (2009). DOI: [10.1002/polb.21695](https://doi.org/10.1002/polb.21695)
- [12] Kim H., Abdala A. A., Macosko C. W.: Graphene/polymer nanocomposites. *Macromolecules*, **43**, 6515–6530 (2010). DOI: [10.1021/ma100572e](https://doi.org/10.1021/ma100572e)
- [13] Potts J. R., Dreyer D. R., Bielawski C. W., Ruoff R. S.: Graphene-based polymer nanocomposites. *Polymer*, **52**, 5–25 (2011). DOI: [10.1016/j.polymer.2010.11.042](https://doi.org/10.1016/j.polymer.2010.11.042)
- [14] Meyer J. C., Geim A. K., Katsnelson M. I., Novoselov K. S., Booth T. J., Roth S.: The structure of suspended graphene sheets. *Nature*, **446**, 60–63 (2007). DOI: [10.1038/nature05545](https://doi.org/10.1038/nature05545)
- [15] Meyer J. C., Geim A. K., Katsnelson M. I., Novoselov K. S., Oberfell D., Roth S., Girit C., Zettl A.: On the roughness of single- and bi-layer graphene membranes. *Solid State Communications*, **143**, 101–109 (2007). DOI: [10.1016/j.ssc.2007.02.047](https://doi.org/10.1016/j.ssc.2007.02.047)
- [16] Gao G., Çağın T., Goddard W. A. III.: Energetics, structure, mechanical and vibrational properties of single-walled carbon nanotubes. *Nanotechnology*, **9**, 184–191 (1998). DOI: [10.1088/0957-4484/9/3/007](https://doi.org/10.1088/0957-4484/9/3/007)